# A new approach for estimating northern peatland gross primary productivity using a satellite-sensor-derived chlorophyll index

A. Harris[1] and J. Dash[2]

Received 21 January 2011; revised 10 June 2011; accepted 6 July 2011; published 1 October 2011.

[1] Carbon flux models that are largely driven by remotely sensed data can be used to estimate gross primary productivity (GPP) over large areas, but despite the importance of peatland ecosystems in the global carbon cycle, relatively little attention has been given to determining their success in these ecosystems. This paper is the first to explore the potential of chlorophyll-based vegetation index models for estimating peatland GPP from satellite data. Using several years of carbon flux data from contrasting peatlands, we explored the relationships between the MERIS terrestrial chlorophyll index (MTCI) and GPP, and determined whether the inclusion of environmental variables such as PAR and temperature, thought to be important determinants of peatland carbon flux, improved upon direct relationships. To place our results in context, we compared the newly developed GPP models with the MODIS (Moderate Resolution Imaging Spectrometer) GPP product. Our results show that simple MTCI-based models can be used for estimates of interannual and intra-annual variability in peatland GPP. The MTCI is a good indicator of GPP and compares favorably with more complex products derived from the MODIS sensor on a site-specific basis. The incorporation of MTCI into a light use efficiency type model, by means of partitioning the fraction of photosynthetic material within a plant canopy, shows most promise for peatland GPP estimation, outperforming all other models. Our results demonstrate that satellite data specifically related to vegetation chlorophyll content may ultimately facilitate improved quantification of peatland carbon flux dynamics.

**Citation:** Harris, A., and J. Dash (2011), A new approach for estimating northern peatland gross primary productivity using a satellite-sensor-derived chlorophyll index, *J. Geophys. Res.*, *116*, G04002, doi:10.1029/2011JG001662.

## 1. Introduction

[2] Despite their limited coverage of the Earth's surface, peatland ecosystems play an important role in the global carbon cycle through the sequestration of atmospheric carbon as peat and the release of carbon gases (carbon dioxide ($CO_2$) and methane ($CH_4$)) through respiration and plant decay. Today most northern peatlands are a significant sink of atmospheric carbon, containing 20%–30% of the global soil carbon pool [*Post et al.*, 1982; *Smith et al.*, 2004]. However, the balance between carbon sequestration and release (as $CO_2$ and $CH_4$) is largely dependent on hydrology and temperature [*Bubier et al.*, 2005; *Bubier*, 1995; *Dise et al.*, 1993; *Moore et al.*, 2006]. Changes in climate may affect the rate of $CO_2$ uptake and the overall carbon dynamics of peatland ecosystems [*Moore*, 1998]; estimates of gross primary productivity (GPP) are thus critical for understanding how these ecosystems respond to climatic changes.

[3] Eddy covariance (EC) methods can measure peatland seasonal and interannual carbon fluxes over long periods of time. While EC techniques have proven to be of great importance in peatland carbon balance modeling efforts [e.g., *Lafleur et al.*, 2003; *Laine et al.*, 2006], these measurements account only for carbon fluxes within the designated flux tower footprint, and the number and geographical distribution of towers across the globe is limited. Consequently, scaling carbon fluxes from flux towers to produce regional and global estimates is challenging. Other attempts to estimate peatland carbon fluxes have concentrated on the development of process-based models, although the difficulties in modeling peatland hydrology mean that there have been relatively few attempts to model carbon exchange in peatlands as compared with other terrestrial ecosystems [e.g., *Frolking et al.*, 2002; *Soegaard et al.*, 2003; *Wang et al.*, 2002; *Yurova et al.*, 2007]. Peatland process-based models, such as the Peatland Carbon Simulator (PCARS) [*Frolking et al.*, 2002; *Lafleur et al.*, 2003], and ecosystem models that have been adapted to northern peatlands, such as the Boreal Ecosystem Productivity Simulator (BEPS) [*Liu et al.*, 1997; *Sonnentag et al.*, 2008] and GUESS-ROMUL [*Yurova et al.*, 2007; *Yurova and Lankreijer*, 2007], have shown promise. However, the applicability of these models at the regional and global scales is particularly challenging because of their

[1]Geography Department, School of Environment and Development, University of Manchester, Manchester, United Kingdom.
[2]School of Geography, University of Southampton, Southampton, United Kingdom.


0148-0227/11/2011JG001662

complexity and requirements for data that are often scarce or unavailable at the appropriate spatial and temporal scales. Carbon flux models that are largely driven by remotely sensed data can be used to estimate gross primary productivity (GPP) over large areas, but despite the importance of peatland ecosystems in the global carbon cycle, relatively little attention has been given to determining their success in these ecosystems.

[4] Many current remote-sensing-based carbon flux models utilize the light use efficiency (LUE) concept of *Monteith* [1972], which suggests that GPP is linearly related to the amount of absorbed photosynthetically active radiation:

$$\mathrm{GPP} = \varepsilon * (f\mathrm{PAR} * \mathrm{PAR}). \quad (1)$$

Where PAR is the incident photosynthetically active radiation, $f$PAR is the fraction of PAR absorbed by the vegetation canopy and $\varepsilon$ is the efficiency with which a plant is able to export or utilize the product of photosynthesis.

[5] The primary advantage of the Monteith model for regional and global carbon flux estimations is that many of the model parameters can be estimated remotely from satellite data. In remote sensing analysis $f$PAR is estimated either as a function of the normalized difference vegetation index (NDVI) [*Prince and Goward*, 1995; *Ruimy et al.*, 1994] or by utilizing physically based models to describe the propagation of light in plant canopies [*Myneni et al.*, 2003]. However, the estimation of the LUE component is often more difficult, since LUE varies spatially across biomes, species and plant functional types [*Gower et al.*, 1999] and temporally across seasons and in response to environmental variations [*Nouvellon et al.*, 2000; *Schwalm et al.*, 2006; *Sims et al.*, 2006b]. Many remote-sensing-based GPP models utilize "look up" tables based on vegetation type to estimate the maximum LUE of a given biome and then adjust this value according to meteorological indicators of environmental stress [*Running et al.*, 2004]. However, there can be substantial errors in the estimation of LUE due to the coarseness of the metrological inputs commonly used to scale LUE and the quality and resolution of the land cover classification on which biome specific maximum LUE values are initially based. A number of studies have suggested that the use of coarse resolution data and look-up table LUE inputs may result in significant errors in the estimation of carbon fluxes [*Heinsch et al.*, 2006; *Zhao et al.*, 2006]. For heterogeneous environments, such as peatlands, the coarseness of such inputs may be particularly problematic, especially given that the land cover classification schemes on which such algorithms are based, often fail to include a peatland land cover category [*Harris and Bryant*, 2009; *Krankina et al.*, 2008].

[6] To try and overcome some of these limitations, several studies advocate a simpler and more direct approach by devising carbon exchange models that are entirely based on remote sensing data (e.g., vegetation indices (VIs)). Such models have the benefit of a continuous output at the spatial resolution of the sensor and are not always reliant on independent meteorological data sets or estimations of LUE [*Rahman et al.*, 2005]. Although the use of VIs in isolation may not be able to track daily fluctuations in carbon exchange, because rapid changes in environmental variables such as PAR, temperature and soil moisture are unlikely to have an immediate impact upon canopy physiology, studies have shown that VIs are able to characterize carbon fluxes integrated over a period of several days. Spectral indices that are related to vegetation greenness such as the normalized difference vegetation index (NDVI) or the enhanced vegetation index (EVI) have been correlated with GPP with varying degrees of success [e.g., *La Puma et al.*, 2007; *Rahman et al.*, 2005; *Sims et al.*, 2006a; *Sims et al.*, 2006b; *Wylie et al.*, 2003]. *Sims et al.* [2006b] reported correlations between EVI and GPP that were as good as or better than more complex algorithms, such as the MODIS GPP product (MOD17), during active photosynthesis. However, the model functions less well for sites dominated by evergreen species and those susceptible to summer drought, primarily because of the lack of a correlation between LUE and vegetation greenness. Recent developments to the *Sims et al.* [2006a] EVI model, through the incorporation of an additional land surface temperature component, have improved predictions of GPP from EVI [*Sims et al.*, 2008].

[7] Despite the recent proliferation of VI-based carbon models, there have been very few attempts to utilize these approaches to model GPP in peatland ecosystems and, like the vast majority of satellite-based GPP models, those that have, rely heavily upon spectral indices derived from the Moderate Imaging Spectrometer (MODIS) [e.g., *Schubert et al.*, 2010]. The use of common MODIS-derived vegetation indices, such as the NDVI and EVI, may be problematic for satellite-based GPP estimation over peatlands because of the narrow red absorption feature and narrow near-infrared reflectance peak, which is commonly observed in dominant peat forming species such as *Sphagnum* mosses [*Bubier et al.*, 1997]. A more general concern about the reliance solely upon MODIS data for satellite-based GPP model development, is the current uncertainty relating to the continuity of the MODIS program, thus there is clearly a motivation to extend knowledge acquired from modeling efforts with the MODIS data sets to other sensor's data.

[8] In this study, we focus on exploring new ways of estimating peatland GPP from alternative sources of satellite data. Our approach is also based upon the logic of *Monteith* [1972] but focuses specifically on the estimation of vegetation chlorophyll content to inform GPP estimations, as opposed to more integrated measures of greenness and structure (e.g., the NDVI and EVI). Previous studies have shown good relationships between chlorophyll content and vegetation stresses, phenology and photosynthetic capacity [e.g., *Gitelson et al.*, 2006; *Jago et al.*, 1999; *Sun et al.*, 2008]. Because chlorophyll is essential for photosynthesis, estimations of chlorophyll content may constitute as a surrogate for the amount of energy that can be transferred for photosynthesis. A number of studies by *Gitelson et al.* [2008, 2006] have demonstrated that remote sensing techniques, developed for chlorophyll retrieval, can be used to estimate GPP in rainfed and irrigated Maize and Soybean crops. Using VIs derived from field spectroradiometry; the product of chlorophyll and photosynthetically active radiation (PAR) was shown to account for 98% of GPP variation in the crop canopies [*Gitelson et al.*, 2005]. Furthermore the relationship was non-species-specific. More recently *Harris and Dash* [2010] were the first to demonstrate strong correlations between EC estimated GPP and a chlorophyll index derived from the Medium Resolution Imaging Spectrometer (MERIS) on board the ENVISAT satellite. The MERIS terrestrial chlorophyll index (MTCI) product effectively combines information on leaf area index and the chlorophyll

concentration of leaves to produce an image of chlorophyll content [*Dash and Curran*, 2004]. The correlations between the MTCI and EC measures of GPP across a range of North American ecosystems was as good as, if not better than, those observed between EC GPP and the MODIS EVI and the more complex MODIS GPP (MOD17) product [*Harris and Dash*, 2010].

[9] In this study, we focus on exploring the relationships between the MTCI and EC measures of GPP in peatland ecosystems. We also develop and test a series of LUE-type regression models based on the MTCI to determine whether the inclusion of environmental variables such as PAR and temperature, improve the direct relationship between MTCI and GPP. To put the results in context, we compare the MTCI model results to those of obtained from the MODIS GPP product (MOD17), which is a satellite-based LUE model commonly use to estimate GPP [*Heinsch et al.*, 2003].

## 2. Methods

### 2.1. Peatland Study Sites

[10] We used carbon flux data from two contrasting Fluxnet Canada Research Network sites: the Mer Bleue peatland (Eastern Peatland) and the Western Peatland. Mer Bleue is a large, open, low-shrub raised bog covering approximately 25 km$^2$ [*Moore et al.*, 2002], located east of Ottawa, Ontario, Canada (45.40°N, 75.52°W). The region has a cool continental climate, with a mean annual temperature of 6°C and an annual rainfall of 732 mm [*Environment Canada*, 2006]. Due to the acidic nutrient-poor nature of the site, the vegetation mainly consists of evergreen species. Overstorey vegetation is dominated by a shrub canopy 20–30 cm high, and the bog surface is dominated by a hummock-hollow microtopography. Hummocks are occupied by the evergreen shrubs *Ledum groenlandicum*, *Kalmia angustifolium*, *Chamaedaphne calyculata* and the deciduous shrub *Vaccinium myrtilloides*. Hollows are approximately 20 cm lower, compose about 25% of the bog surface and have a sparser coverage of *L. groenlandicum, K. angustifolium*, and *C. calyculata*. The bog ground cover is dominated by *Sphagnum* mosses [*Moore et al.*, 2002]. The growing season is from May to September [*Lafleur et al.*, 2003] with an average temperature during this period of 17°C [*Environment Canada*, 2006]. The Western Peatland is a moderately rich treed fen located in the La Biche River area in Alberta, Canada (54.95°N, 112.46°W). The climate of the region is classified as continental with a mean annual temperature of 2.1°C and an annual rainfall of 382 mm [*Environment Canada*, 2006]. In contrast to Mer Bleue, the vegetation is largely composed of deciduous species. Stunted trees of *Picea maiana* and *Larix laricina* dominate the vegetation, with high abundance of the shrub *Betula pumila*, and a wide range of moss species including *Sphagnum*, brown and feather mosses [*Syed et al.*, 2006]. The growing season at the Western Peatland is from May to October [*Syed et al.*, 2006]. The avaerage tempertaure during this period is 12°C [*Environment Canada*, 2006]. Both sites are representative of peatlands in the boreal region.

### 2.2. Satellite Data

[11] Table 1 displays the sensor specifications for the MODIS and MERIS instruments. The spatial location of both the MERIS and MODIS data were carefully chosen to maximize the area of peatland covered by each 1 km pixel. At Mer Bleue, the EC tower is located approximately 300 m from the margin of the bog and has an ~1 km footprint. Approximately 80% of the flux emanates from within 200 m of the tower [*Connolly et al.*, 2009], which is largely dominated by hummocks [*Moore et al.*, 2006]. Inspection of the MERIS pixel footprint using Landsat data together with high resolution data obtained from Google Earth™, indicated that approximately 80% of the MERIS pixel was dominated by peatland land cover, deemed representative of the flux tower footprint, with the remainder covering a narrow band of mixed forest and cattail marsh to the south of the pixel (Figure 1). The EC tower footprint at the Western Peatland site ranges from 1.5 to 2 km in all directions except north where the fetch is ~1 km. The flux tower footprint is dominated by relatively homogeneous vegetation [*Syed et al.*, 2006] and is located toward the western edge of both the MERIS and MODIS pixels.

#### 2.2.1. Medium Resolution Imaging Spectrometer (MERIS) Data

[12] The 1 km spatial resolution 8-day composites of MERIS MTCI were downloaded from the UK Natural Environment Research Council Earth Observation Data Centre (NERC NEODC; http://www.neodc.rl.ac.uk). The MTCI is a ratio of the difference in reflectance between band 10 and band 9 and the difference in reflectance between band 9 and band 8 of the MERIS standard band setting using the following equation [*Dash and Curran*, 2004]:

$$\begin{aligned} \mathrm{MTCI} &= \rho_{\mathrm{Band10}} - \rho_{\mathrm{Band9}} / \rho_{\mathrm{Band9}} - \rho_{\mathrm{Band8}} \\ &= \rho_{753.75} - \rho_{708.75} / \rho_{708.75} - \rho_{681.25}, \end{aligned} \quad (2)$$

where $\rho_{753.75}$, $\rho_{708.75}$, $\rho_{681.25}$ are reflectance in the center wavelengths of the MERIS standard band setting. The MTCI data were composited from standard Level 2 reduced resolution (geophysical) products using an arithmetic mean and a flux conversion resampling [*Curran et al.*, 2007].

[13] To determine how representative the 1 km MERIS MTCI data were of the tower footprints at each site, we obtained MTCI data from two years of full resolution (300m) MERIS data. We identified the 300 m pixels that were most representative of the 1 km pixel extents and extracted the standard level 2 MTCI values (Figure 1). For each site, we compared the amplitude and seasonal patterns of the 300 m and 1 km MTCI data.

#### 2.2.2. Moderate Resolution Imaging Spectrometer (MODIS) Data

[14] The 1 km 8-day composites of MODIS Land Surface Temperature (LST; collection 5.0 data sets), *f*PAR and MOD17 GPP data (collection 5.1 data sets) were acquired from the Oak Ridge National Laboratory's Distributed Active Archive Centre (DAAC) (http://www.modis.ornl.gov/modis/index.cfm). We used the MODIS quality control flags to select data with low cloud cover and listed as "Good Quality." All LST data were derived from the Terra satellite, which has a morning overpass time between 1000 and 1100 h. The MOD17 GPP product is calculated using a LUE type model:

$$GPP = \varepsilon_{\max} * m(T_{\min}) * m(VPD) * fPAR * SWrad * 0.45, \quad (3)$$

**Table 1.** Specifications of MERIS (Medium Resolution Imaging Spectrometer) and MODIS (Moderate Resolution Imaging Spectroradiometer) Sensors

| Specifications | MERIS | | | MODIS | | |
|---|---|---|---|---|---|---|
| Name | Medium Resolution Imaging Spectrometer | | | Moderate Resolution Imaging Spectroradiometer | | |
| Satellite | ENVISAT | | | Terra/Aqua | | |
| Swath Width | 1150 km | | | 2330 km | | |
| Revisit Period | ~3 days | | | daily | | |
| Spatial Resolution at Nadir | 1200 m × 1004 m (reduced resolution)<br>290 m × 260 m (full resolution) | | | 250 m (bands 1–2)<br>500 m (bands 3–7)<br>1000 m (bands 8–36) | | |
| | Total of 15 bands spanning the VIS and NIR | | | Total of 36 bands spanning the VIS, NIR, SWIR (shortwave infrared) and LWIR (long wave infrared) | | |
| Spectral Resolution | No. | Band Centre[a] | Band Width (nm) | No. | Band Centre[a] | Band Width (nm) |
| | 1 | 412.5 | 10 | 1 | 645 | 50 |
| | 2 | 442.5 | 10 | 2 | 858.5 | 35 |
| | 3 | 490 | 10 | 3 | 469 | 20 |
| | 4 | 510 | 10 | 4 | 555 | 20 |
| | 5 | 560 | 10 | 5 | 1240 | 20 |
| | 6 | 620 | 10 | 6 | 1640 | 24 |
| | 7 | 665 | 10 | 7 | 2130 | 50 |
| | 8 | 681.25 | 7.5 | 8 | 412.5 | 15 |
| | 9 | 708.75 | 10 | 9 | 443 | 10 |
| | 10 | 753.75 | 7.5 | 10 | 488 | 10 |
| | 11 | 760.63 | 3.75 | 11 | 531 | 10 |
| | 12 | 778.75 | 15 | 12 | 551 | 10 |
| | 13 | 865 | 20 | 13 | 667 | 10 |
| | 14 | 865 | 10 | 14 | 678 | 10 |
| | 15 | 900 | 10 | 15 | 748 | 10 |
| | | | | 16 | 869.5 | 15 |
| | | | | 17 | 905 | 30 |
| | | | | 18 | 936 | 10 |
| | | | | 19 | 940 | 50 |
| | | | | 20 | 3.750 | 180 |
| | | | | 21 | 3.959 | 60 |
| | | | | 22 | 3.959 | 60 |
| | | | | 23 | 4.050 | 60 |
| | | | | 24 | 4.465 | 65 |
| | | | | 25 | 4.515 | 67 |
| | | | | 26 | 1.375 | 30 |
| | | | | 27 | 6.715 | 360 |
| | | | | 28 | 7.325 | 300 |
| | | | | 29 | 8.550 | 300 |
| | | | | 30 | 9.730 | 300 |
| | | | | 31 | 11.180 | 500 |
| | | | | 32 | 12.020 | 500 |
| | | | | 33 | 13.335 | 300 |
| | | | | 34 | 13.635 | 300 |
| | | | | 35 | 13.935 | 300 |
| | | | | 36 | 14.235 | 300 |

[a]Data for MERIS and MODIS bands 1 to 19 are in nm; data for MODIS bands 20 to 36 are in $\mu$m. Greyed areas indicate bands spanning the VIS and NIR wavelength range common to both sensors.

where $\varepsilon_{max}$ is the maximum LUE and the scalers m($T_{min}$) and m(VPD) reduce $\varepsilon_{max}$ under conditions of low temperature and high vapor pressure deficit (VPD). $f$PAR is the fraction of PAR absorbed by the vegetation canopy and SWrad is shortwave radiation. VPD and SWrad are obtained from coarse scale meteorological data sets from the NASA Data Assimilation Office (DAO; http:gmao.gsfc.nasa.gov/), and $\varepsilon_{max}$ is obtained from LUE look-up tables on the basis of biome type [*Heinsch et al.*, 2003].

### 2.3. Tower-Based Carbon Flux Data and Environmental Variables

[15] Flux tower data were obtained from the FLUXNET Canada website (http://www.fluxnet-canada.ca/). Based on the concurrent availability of MTCI and tower data, we obtained gap-filled 30 min values of GPP (taken as equivalent to ecosystem productivity; GEP; *Moore et al.*, 2006), incoming photosynthetically active radiation (PAR), air temperature (AT), and water table depth (WTD) from January 2003 to December 2006 for Mer Bleue and from January 2004 to December 2005 for the Western Peatland. All variables were averaged both monthly and over 8-day periods to be consistent with both long-term climatic data sets and the satellite data products used. Only data from the period when active photosynthesis was occurring were used for analysis. We defined this period by selecting data only from periods when PAR was greater than 10 umol $m^{-2}$ $s^{-1}$ and GPP greater than zero. In addition, because of the lack of quality control flags to accompany the MTCI data, when developing and comparing satellite-based models, we only

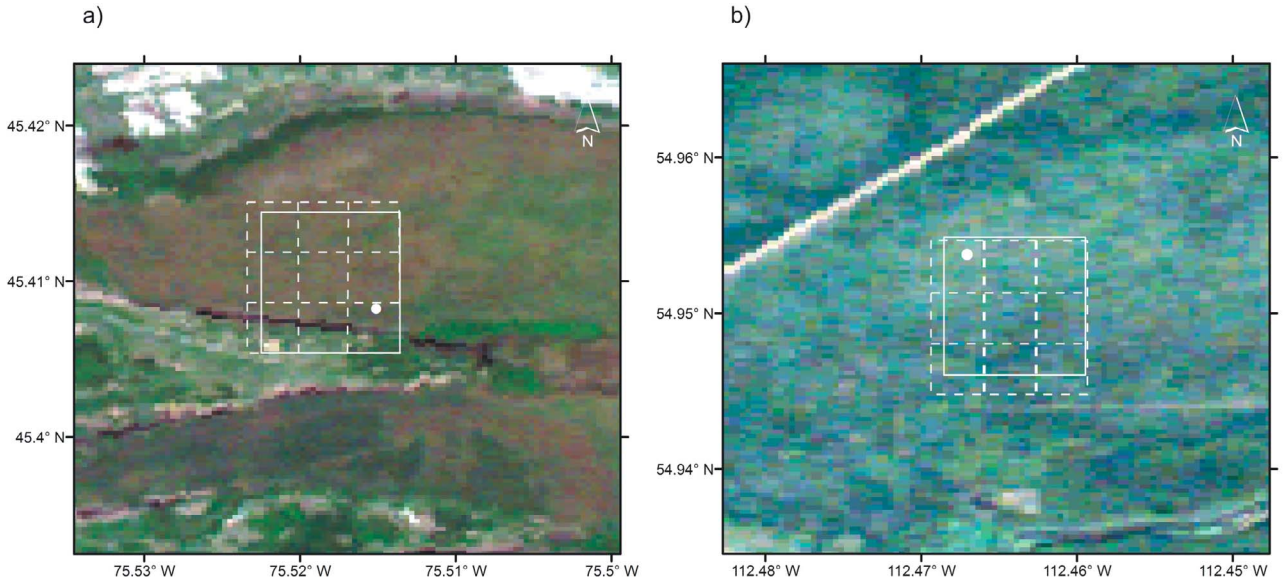


**Figure 1.** A schematic diagram indicating the location of the 1 km (solid lines) and 300 m (dashed lines) MTCI pixels used in the study, shown in relation to the flux tower sites (white circles) for (a) Mer Bleue and (b) the Western Peatland. A Landsat scene is displayed beneath the pixel locations for context (red = band 3, green = band 2, blue = band 1). Note that the MTCI 1 km pixels actually measure 700 m × 1 km at these sites due to the geographic lat/lon projection of the data. The product is available at 1 × 1 km spatial resolution at the equator.

used data when the 8-day average daytime AT was greater than 5°C [*Arora and Boer*, 2005] to ensure avoidance of snow covered pixels. Positive values of GPP represent a net flux into the ecosystem. Full details of the EC system, quality assurance and gap-filling procedures can be found in *Lafleur et al.* [2001, 2005, 2003] for Mer Bleue and in *Syed et al.* [2006] for the Western Peatland.

### 2.4. Calculation of Tower-Based Light Use Efficiency (LUE)

[16] Calculation of LUE requires an estimation of the absorbed photosynthetically active radiation (APAR). APAR was calculated as a function of the total daily incident PAR recorded at the EC tower (where PAR is greater than 10 umol $m^{-2}$ $s^{-1}$) and *f*PAR is the corresponding MODIS 8-day *f*PAR value using the following equation:

$$\mathrm{APAR} = f\mathrm{PAR} * \mathrm{PAR}. \quad (4)$$

Using Beer's Law, *Connolly et al.* [2009] showed that MODIS *f*PAR data for both Mer Bleue and the Western Peatland are representative of *f*PAR values derived from field measures of leaf area index (LAI), despite the lack of a distinctive peatland land cover category in the MODIS algorithm. We only used *f*PAR values flagged as excellent quality in the calculation of APAR. LUE was then calculated using the following formula:

$$\mathrm{LUE} = \mathrm{GPP}/\mathrm{APAR}. \quad (5)$$

### 2.5. Model Development

[17] A series of MTCI-based linear regression models were developed to explore a new approach of estimating peatland GPP from satellite data. Chlorophyll content is intrinsically related to the process of photosynthesis; we therefore first investigated the possibility of estimating GPP directly from the MTCI:

$$\mathrm{GPP} = a(\mathrm{MTCI}) + b. \quad (6)$$

[18] The use of environmental variables or proxy environmental variables, that are known to have an important influence of plant carbon exchange processes, alongside satellite-based measurements of canopy vitality (e.g., chlorophyll content, greenness and *f*PAR), have previously been shown to improve correlations with in situ estimations of GPP [e.g., *Gitelson et al.*, 2006; *Schubert et al.*, 2010; *Sims et al.*, 2008]. Based on these findings, and the LUE concept of *Monteith* [1972], we investigated linear relationships between peatland GPP and the product of MTCI and PAR, the product of MTCI and *f*PAR and the product of MTCI, *f*PAR and PAR i.e., the product of MTCI and APAR:

$$\mathrm{GPP} = a(\mathrm{MTCI} \times \mathrm{PAR}) + b, \quad (7)$$

$$\mathrm{GPP} = a(\mathrm{MTCI} \times f\mathrm{PAR}) + b, \quad (8)$$

$$\mathrm{GPP} = a(\mathrm{MTCI} \times f\mathrm{PAR} \times \mathrm{PAR}) + b, \quad (9)$$

where $a$ and $b$ are the slope and intercept in a linear model ($y = ax + b$). Finally, based on previously reported strong correlations between GPP and the product of greenness VIs and land surface temperature (LST) [*Sims et al.*, 2008], we examined the correlation between peatland GPP and the product of MTCI and MODIS LST:

$$\mathrm{GPP} = a(\mathrm{MTCI} \times \mathrm{LST}) + b. \quad (10)$$

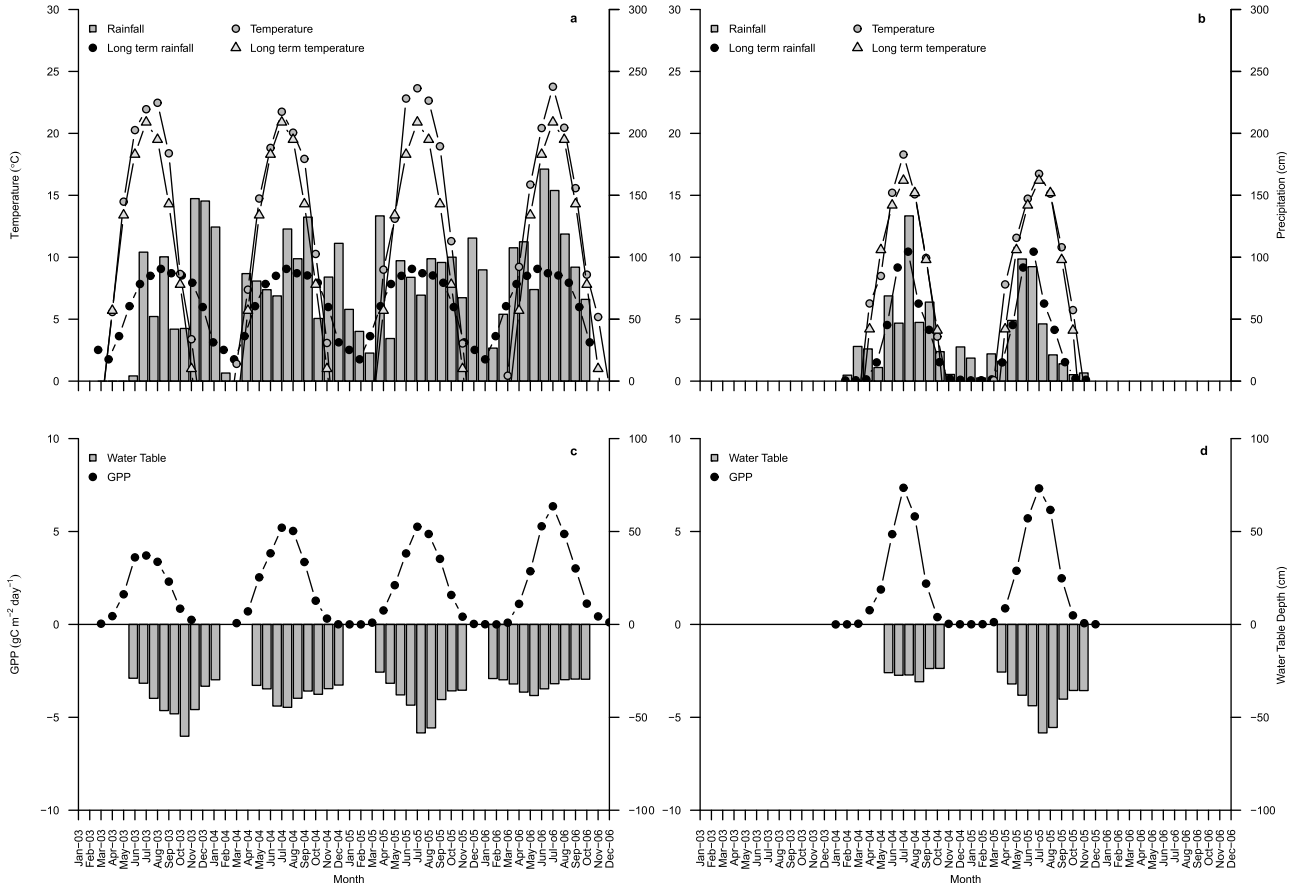


**Figure 2.** Seasonal monthly pattern of precipitation, temperature, gross primary productivity and water table depth below a hummock surface, during the growing season for Mer Bleue (a and c) and the Western Peatland (b and d). Thirty-year (1971–2000) normals of temperature and rainfall are also presented for comparison purposes.

[19] For each model, the root mean square error (RMSE) of GPP estimation was obtained for each site and across sites using the leave-one-out cross validation method [*Lachenbruch and Mickey*, 1968] because of the relatively small sample size. This approach involved (1) removing one data point from the data set, (2) calculating the relationship for the remaining points, (3) predicting GPP for the left-out data point and (4) repeating for all points. The root mean square error was used to compare predicted with EC tower-measured GPP:

$$RMSE = \sqrt{\frac{\left(GPP_t - GPP_p\right)^2}{n}}, \tag{11}$$

where $GPP_t$ is the GPP measured at the tower, $GPP_p$ is the predicted GPP using leave-one-out method and n is the number of samples.

## 3. Results

### 3.1. Interannual and Seasonal Dynamics of Peatland Ecosystem Components

[20] Long-term data suggest a seasonal trend in rainfall at Mer Bleue with the summer months (June–August) often being the wettest (Figure 2a). However, the rainfall pattern during 2003 to 2005 was far less pronounced than either the long-term average for the site or the rainfall pattern observed at the Western Peatland (Figure 2b). The growing season in 2003 (May–September) was characterized by very low rainfall, with three months out of the five month period recording only half of the long-term rainfall average. In contrast the fall was unseasonably wet with over seven times more rain falling than normal from October to December 2003. A similar pattern of above average rainfall was also observed during the fall of 2006. Differences in rainfall were mirrored in the water-table position and in the interannual pattern in GPP, where photosynthetic rates were substantially lower during the 2003 growing season (Figure 2c). GPP reached its peak in July although the photosynthetic rates were on average lower than those observed at the Western Peatland.

[21] During 2004 and 2005 the Western Peatland was characterized by clear seasonal patterns in both rainfall and temperature (Figure 2b). Monthly average rainfall was greatest during the summer months with most rainfall falling in July and June (2004 and 2005, respectively). Total annual recorded rainfall was higher in 2004 than in 2005, with several months receiving above average rainfall. Rainfall

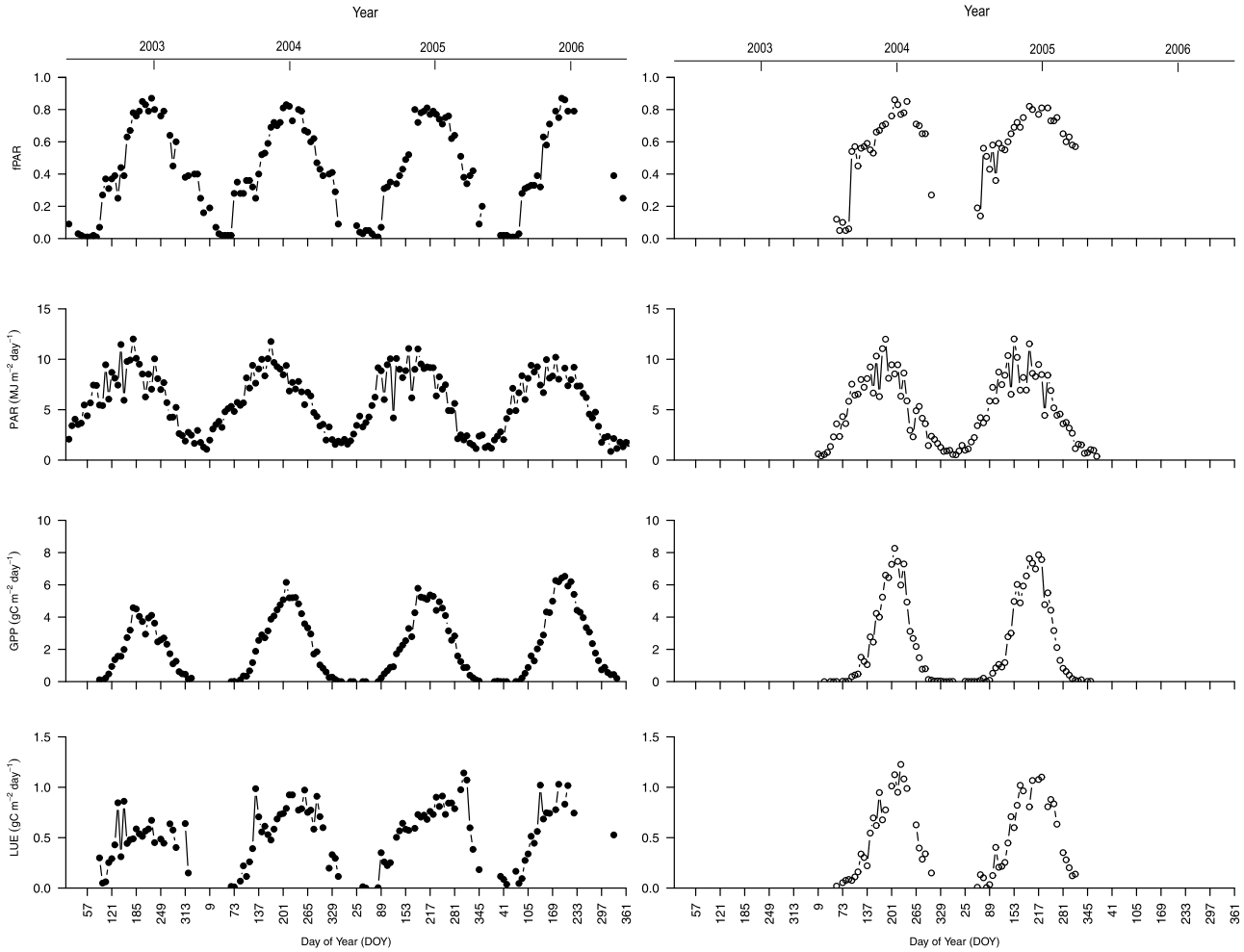


**Figure 3.** Eight-day temporal profiles of the fraction of photosyntehtically active radiation (*f*PAR), incoming photosynthetically active radiation (PAR), gross primary productivity (GPP) and light use efficiency (LUE) for Mer Bleue (a, c, e and g, respectively) and the Western Peatland (b, d, f and h, respectively). All available data are included in the plots; gaps are indicative of missing data.

and temperature fluctuations were both reflected in the water table levels and in tower GPP (Figure 2d). In both years daily photosynthetic rates were greatest in June and July, coincident with both the highest seasonal temperatures and the greatest amount of rainfall.

### 3.2. Peatland Light Use Efficiency (LUE)

[22] We analyzed the relationship between GPP and APAR to determine the extent of variation in LUE within and between the peatland sites, and thus the importance of LUE in the estimation of peatland GPP. As incoming PAR, *f*PAR and GPP are the main constituents of derived measures of LUE, we plotted 8-day averages of these variables and LUE against the day of year (DOY) for each site (Figure 3).

[23] The plots of MODIS *f*PAR and in situ incoming PAR show the presence of a strong seasonal pattern across all years and for both sites (Figures 3a–3d). Maximum values of MODIS *f*PAR were similar between years and between the two peatland sites. Large increases in the *f*PAR values at the beginning of the year, for both sites, are indicative of snowmelt. Mid-summer *f*PAR values for Mer Bleue are similar to those reported by *Connolly et al.* [2009] who found good correspondence between *f*PAR derived from field measurements and MODIS *f*PAR for the Mer Bleue peatland, despite the lack of a peatland class in the IGBP classification scheme, which underlies the MODIS *f*PAR algorithm. Values of incoming PAR were also similar at Mer Bleue and the Western Peatland, with daily average maximum values between 10 and 12 MJ m$^{-2}$ day$^{-1}$ for all years studied.

[24] As expected the LUE parameter for both sites followed a similar seasonal pattern to that of *f*PAR, PAR and GPP, but there were clear differences in LUE between the sites and years studied (Figures 3g–3h). Maximum values of LUE were on average higher at the Western Peatland than that at Mer Bleue during peak growing season. At the Western Peatland LUE was similar between the two years studied, but at Mer Bleue LUE was significantly reduced during the summer of 2003 (DOY 185–257) compared to the same time period in 2004, 2005 and 2006 (Figure 3g). A difference in the timing of maximum LUE occurrence is also present in 2005 where LUE continued to increase until late October (DOY 297) before sharply decreasing. This change in pattern may be a consequence of the higher than

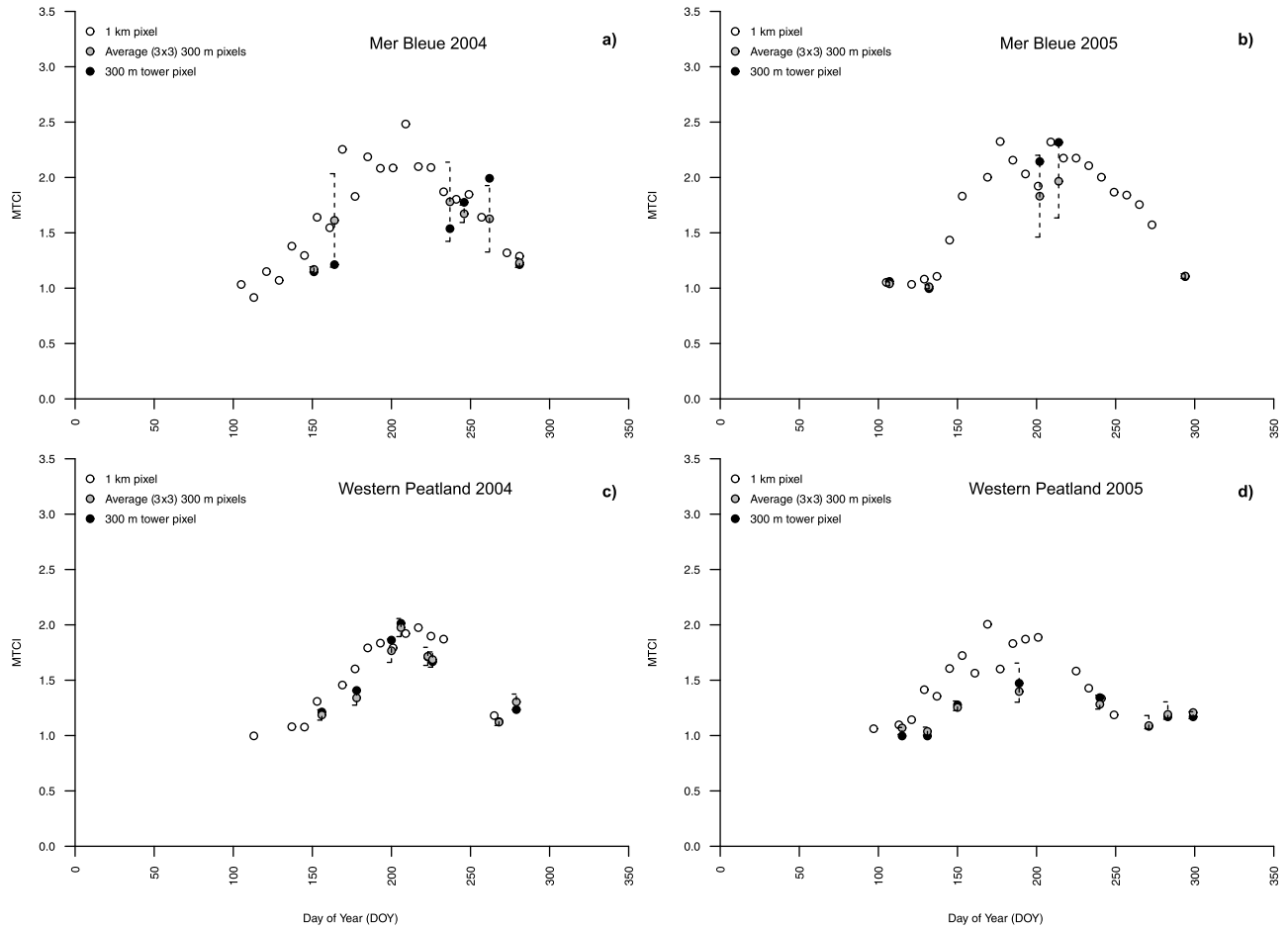


**Figure 4.** Time series of 300 m and 1 km MTCI data for (a and b) Mer Bleue and (c and d) the Western Peatland. The 300 m data points represent the mean of the 300 m pixels corresponding to the 1 km pixel footprint and the pixel closest to the flux tower. Error bars represent +/− 1 s.d. of the mean. For the 1 km data the composite day of the year is used, and for the 300 m data the day of data acquisition is used.

average temperatures experienced at Mer Bleue during the summer of 2005 (Figure 2a).

### 3.3. Seasonal Dynamics of the MTCI and Peatland GPP

[25] Despite the paucity of data, due to the availability of cloud free full resolution MERIS imagery, a comparison of the 300 m resolution and 1 km MTCI data for the years 2004 and 2005 illustrated similar seasonal patterns and amplitudes of MTCI at both sites (Figure 4). The full resolution data indicated that spatial variation in MTCI values within the 1 km pixels varied between sites, with the Mer Bleue peatland exhibiting the greatest spatial heterogenity, at the 300 m scale (Figure 4). Nevertheless, the seasonality and amplitude of the 1 km MTCI values showed a close resemblance to the 300 m data pixels closest to each of the flux towers (Figure 4), thus confirming that the 1 km data were representative of the peatland vegetation within the fetch of the flux towers.

[26] For both peatland sites there was generally good agreement between seasonal tower GPP dynamics and the MTCI (Figure 5). Mid-summer MTCI values were often higher at Mer Bleue than at the Western Peatland. Although the MTCI was able to track the seasonal patterns in ecosystem productivity, the lower GPP values observed at Mer Bleue in 2003, as compared to the remaining years, were not reflected by lower values of MTCI (Figure 5a).

### 3.4. Environmental Controls on Peatland GPP and Correlations With Model Variables

[27] Table 2 shows the relationships between individual variables used in model development (i.e., PAR, LST, $f$PAR and MTCI) and environmental variables thought to exert a controlling influence over peatland GPP (i.e., AT and WTD). Of the three additional variables used to develop the basic MTCI model, LST and $f$PAR showed most promise as proxy variables of the two major controls on GPP. Both LST and $f$PAR were significantly correlated with air temperature (AT) for all years and at both sites, although the strength of the correlation varied between years. Results show that $f$PAR was also significantly correlated with the depth to the water table (WTD) for all years and at both sites, whereas the strength of correlation between WTD and LST was weaker and often not significant (Table 2). PAR showed the least promise for enhancing the basic MTCI model due to weak and often non significant relationships with both of the major controls of GPP (i.e., AT and WTD) and with GPP itself.

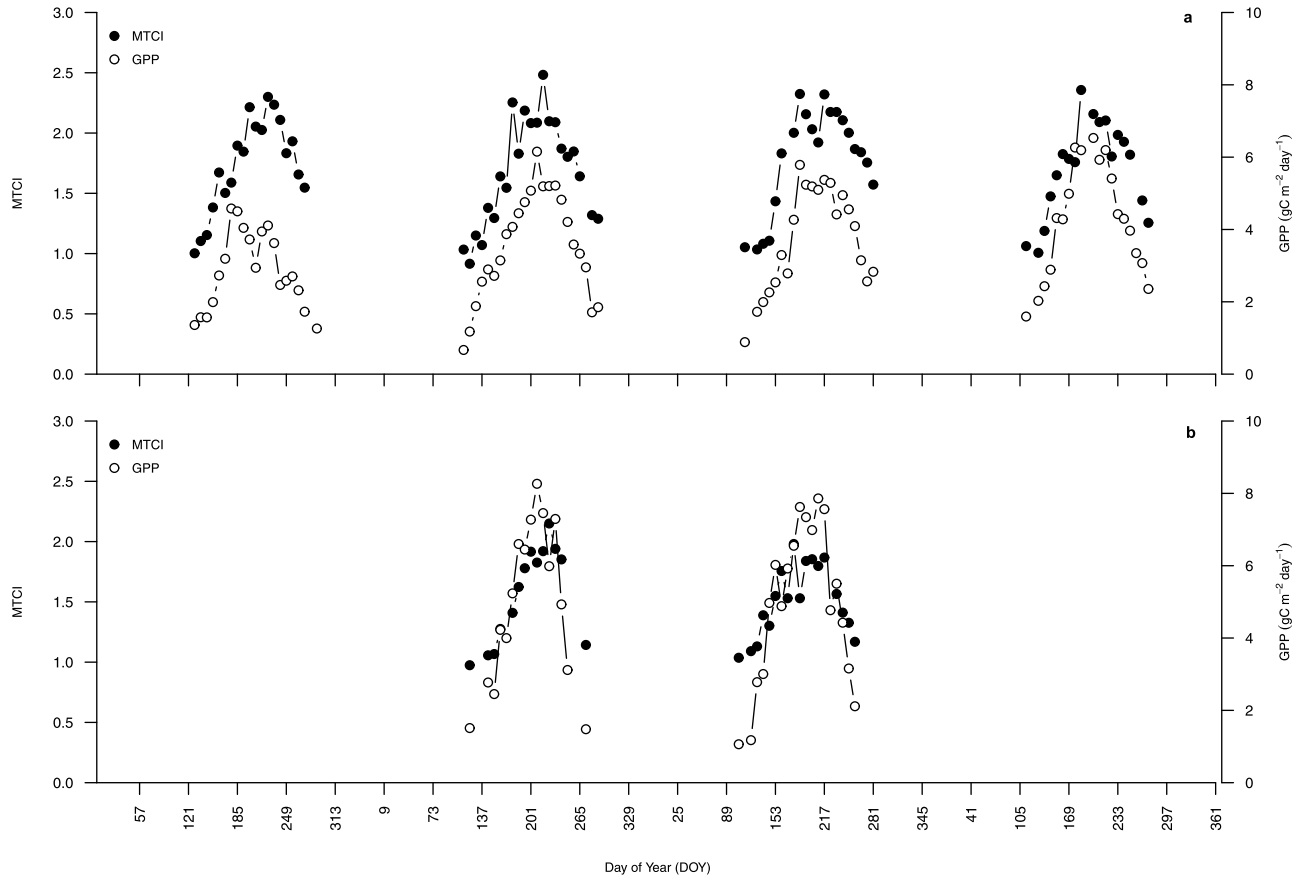


**Figure 5.** Interannual and seasonal variations in the MERIS terrestrial chlorophyll index (MTCI) and gross primary productivity (GPP) at (a) Mer Bleue, 2003–2006; and (b) Western Peatland, 2004–2005. Only data from the growing season, defined as the period when GPP is >0 gC m$^{-2}$ day$^{-1}$ and temperature is >5°C, are used.

[28] We also determined the degree of independence between the MTCI and the additional variables used in the MTCI models by examining the correlations between the MTCI and PAR, LST and *f*PAR. For both sites and all years the MTCI was only weakly correlated with LST and showed no significant correlation with PAR (Table 2). As expected, there were significant correlations between the MTCI and *f*PAR, although the strength of these correlations varied between sites, and importantly between different years at the same site, suggesting that the two variables are indicative of different, but sometimes related, vegetation physiological attributes (Table 2). The lack of strong consistent correlations between the MTCI and PAR, LST and *f*PAR, coupled with the significant correlations observed between a number of these variables and the major controls on GPP, suggest that these variables may be able to provide some additional independent information.

### 3.5. Model Results

[29] Strong linear relationships were observed between GPP and a number of the models tested (Table 3 and Figure 6). The MTCI was strongly correlated with GPP for both peatland sites, for individual years and across all years (Figure 6a). The exception to this was at the Mer Bleue peatland in 2003, where the coefficient of determination was notably lower (Table 3). The addition of LST to the basic MTCI model generally did not significantly improve model performance for individual years or when all years were combined at either of the sites, because GPP was often more strongly correlated with the MTCI than with LST during the growing season (Table 3 and Figure 6b). Again, the exception to this was the year 2003 at Mer Bleue, where the addition of LST to the MTCI model significantly improved model performance for that year ($r^2$ = 0.46 and $r^2$ = 0.74, respectively) primarily due to the presence of a stronger correlation between GPP and LST during that time period (Table 2). The product of MTCI and PAR was also able to explain more variation in GPP than the simple MTCI model for 2003 at Mer Bleue. However, the coefficients of determination for the other years tested at each of the peatlands, and when all years were combined, were reduced relative to the basic MTCI model because of the lack of significant relationships between GPP and PAR at either site (Table 2, Table 3 and Figure 6c). The addition of *f*PAR to the basic MTCI model resulted in small increases in the level of explained variance in GPP at both sites, relative to both the MTCI model and the use of *f*PAR alone (Table 2, Table 3 and Figure 6d), although the greatest improvements were observed when both *f*PAR and PAR were incorporated into the initial MTCI model (Table 3 and Figure 6e). However,

**Table 2.** Regression Statistics for Linear Relationships for the MTCI and Environmental Variables at the Mer Bleue and Western Peatland Sites, Against PAR, LST and *f*PAR[a]

| | | GPP ($gC\ m^{-2}\ day^{-1}$) | AT (°C) | WTD (cm) | MTCI |
|---|---|---|---|---|---|
| Site | Time Period | $r^2$ | $r^2$ | $r^2$ | $r^2$ |
| | | *Mer Bleue* | | | |
| PAR | 2003 | 0.26 | ns | ns | ns |
| | 2004 | ns | 0.20 | ns | ns |
| | 2005 | ns | ns | 0.29 | ns |
| | 2006 | ns | ns | ns | ns |
| | 2003–2006 | 0.07 | 0.06 | ns | ns |
| LST | 2003 | 0.77 | 0.57 | ns | 0.37 |
| | 2004 | 0.36 | 0.39 | 0.20 | 0.24 |
| | 2005 | 0.52 | 0.67 | ns | 0.47 |
| | 2006 | 0.30 | 0.35 | 0.22 | 0.28 |
| | 2003–2006 | 0.35 | 0.45 | 0.07 | 0.31 |
| *f*PAR | 2003 | 0.60 | 0.44 | 0.38 | 0.48 |
| | 2004 | 0.79 | 0.52 | 0.52 | 0.79 |
| | 2005 | 0.78 | 0.66 | 0.50 | 0.83 |
| | 2006 | 0.86 | 0.65 | ns | 0.80 |
| | 2003–2006 | 0.93 | 0.55 | 0.33 | 0.67 |
| | | *Western Peatland* | | | |
| PAR | 2004 | ns | 0.47 | ns | ns |
| | 2005 | ns | 0.41 | 0.25 | ns |
| | 2004–2005 | 0.15 | 0.43 | ns | ns |
| LST | 2004 | 0.29 | 0.59 | 0.24 | ns |
| | 2005 | 0.56 | 0.58 | ns | 0.32 |
| | 2004–2005 | 0.38 | 0.57 | ns | 0.16 |
| *f*PAR | 2004 | 0.63 | 0.23 | 0.21 | 0.76 |
| | 2005 | 0.67 | 0.41 | 0.50 | 0.55 |
| | 2004–2005 | 0.63 | 0.39 | 0.30 | 0.65 |

[a]All values are taken from the growing season defined as the period when GPP is >0 $gC\ m^{-2}\ day^{-1}$ and air temperature is >5°C; ns = not significant at the $P < 0.05$ level.

while the product of MTCI, *f*PAR and PAR was able to explain an additional ~15% of the variability in GPP at the Western Peatland when all years were combined, this more complex model only explained an additional ~4% of GPP variation at the Mer Bleue site, when compared to using MTCI alone. The strength of correlations between GPP and the MODIS GPP product were similar to those reported for a number of the MTCI models tested (Table 3 and Figure 6f), although the product of MTCI, PAR and *f*PAR was able to explain more of the variation in GPP at the Western Peatland, than the MODIS GPP product ($r^2 = 0.91$ and $r^2 = 0.77$, respectively). In a similar vein to many of the MTCI models, the coefficient of determination for the MODIS GPP model was also lower at the Mer Bleue site for 2003, relative to the other years.

[30] While the strength of the model correlations was similar between the two peatlands, the slope of the relationship differed (Table 3 and Figure 6). Slopes were similar between years within a given site, apart from the slope of the 2003 relationship at Mer Bleue where the slope of the regression line between GPP and all models was lower in comparison to other years. For all of the models, the slope of the regression line was always greater for the Western Peatland than for Mer Bleue. The MODIS GPP product behaved in a similar manner to the MTCI models, although

**Table 3.** Linear Regressions for GPP ($gC\ m^{-2}\ day^{-1}$) at Mer Bleue and Western Peatland Against the Product MTCI and Land Surface Temperature (MODIS LST); the Product of MTCI and Photosynthetically Active Radiation (PAR); the Product of MTCI and Fraction of Absorbed Photosynthetically Active Radiation (MODIS *f*PAR); the Product of MTCI, MODIS *f*PAR, and PAR; and the MODIS GPP product (MOD17)[a]

| | *x* = MTCI | | | *x* = MTCI X LST | | | *x* = MTCI X PAR | | | *x* = MTCI X *f*PAR | | | *x* = MTCI X *f*PAR × PAR | | | MODIS GPP | | |
|---|---|---|---|---|---|---|---|---|---|---|---|---|---|---|---|---|---|---|
| | $r^2$ | *a* | *b* | $r^2$ | *a* | *b* | $r^2$ | *a* | *b* | $r^2$ | *a* | *b* | $r^2$ | *a* | *b* | $r^2$ | *a* | *b* |
| | | | | | | | | | *Mer Bleue* | | | | | | | | | |
| 2003 | 0.46 (19) | 1.81 | −0.21 | 0.74 (17) | 0.07 | 0.15 | 0.68 (19) | 0.19 | 0.22 | 0.59 (17) | 1.54 | 1.10 | 0.82 (17) | 0.20 | 0.96 | 0.75 (20) | 0.62 | 0.05 |
| 2004 | 0.82 (22) | 3.03 | −1.52 | 0.81 (22) | 0.10 | −0.06 | 0.66 (22) | 0.26 | 0.09 | 0.85 (21) | 2.61 | 0.63 | 0.84 (21) | 0.29 | 0.94 | 0.83 (23) | 0.78 | 0.31 |
| 2005 | 0.87 (20) | 3.14 | −1.84 | 0.86 (20) | 0.11 | −0.19 | 0.68 (20) | 0.23 | 0.26 | 0.88 (20) | 2.68 | 0.49 | 0.91 (20) | 0.28 | 0.94 | 0.81 (21) | 0.82 | 0.15 |
| 2006 | 0.82 (18) | 3.72 | −2.06 | 0.76 (18) | 0.11 | −0.19 | 0.81 (18) | 0.34 | −0.30 | 0.92 (11) | 3.14 | 0.80 | 0.95 (10) | 0.35 | 1.03 | 0.94 (19) | 0.91 | 0.11 |
| 2003–2006 | 0.66 (79) | 2.90 | −1.37 | 0.68 (77) | 0.09 | 0.01 | 0.58 (79) | 0.24 | 0.24 | 0.70 (69) | 2.39 | 0.80 | 0.75 (68) | 0.27 | 1.00 | 0.72 (83) | 0.78 | 0.17 |
| 2004–2006 | 0.79 (60) | 3.20 | −1.67 | 0.76 (60) | 0.10 | −0.07 | 0.64 (60) | 0.26 | 0.22 | 0.84 (52) | 2.74 | 0.63 | 0.86 (51) | 0.30 | 0.94 | 0.85 (63) | 0.84 | 0.17 |
| | | | | | | | | | *Western Peatland* | | | | | | | | | |
| 2004 | 0.77 (14) | 5.05 | −2.78 | 0.88 (14) | 0.20 | −1.42 | 0.83 (14) | 0.48 | −1.27 | 0.74 (13) | 4.66 | −0.29 | 0.94 (13) | 0.56 | −0.38 | 0.81 (16) | 1.11 | −0.66 |
| 2005 | 0.77 (18) | 6.71 | −5.17 | 0.8 (17) | 0.21 | −1.10 | 0.78 (18) | 0.54 | −1.77 | 0.86 (16) | 7.37 | −3.08 | 0.89 (16) | 0.63 | −0.96 | 0.74 (19) | 1.18 | −0.10 |
| 2004–2005 | 0.75 (32) | 5.72 | −3.75 | 0.8 (31) | 0.20 | −0.97 | 0.78(32) | 0.50 | −1.47 | 0.77 (29) | 5.88 | −1.26 | 0.91 (29) | 0.59 | −0.63 | 0.77 (35) | 1.14 | −0.82 |

[a]All values are taken from the growing season, defined as the period when GPP is >0 $gC\ m^{-2}\ day^{-1}$ and air temperature is >5°C. The italic *a* and *b* represent constants for the linear regression models ($y = ax + b$). Numbers in parentheses represent the number of data points used in the regression.

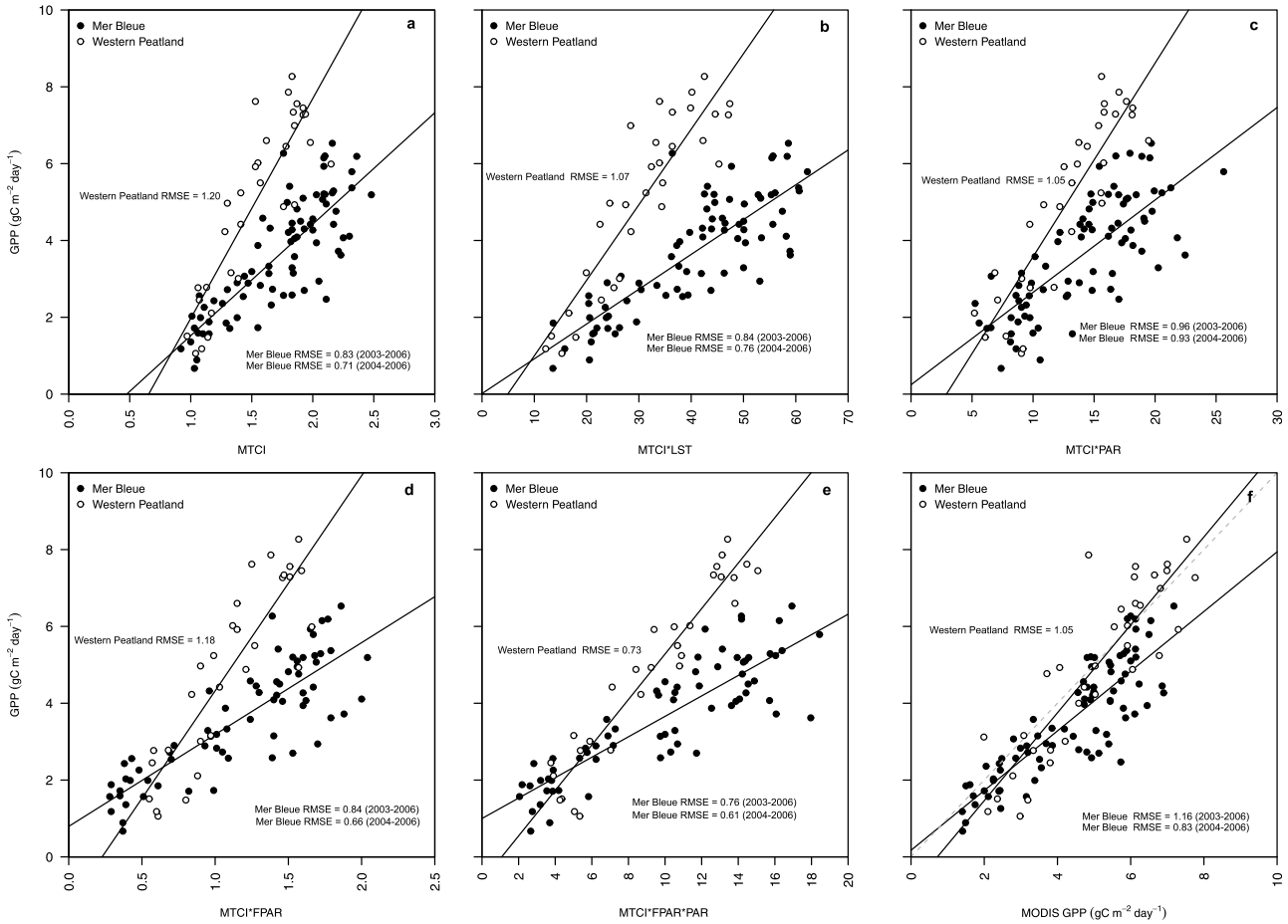


**Figure 6.** Gross primary productivity (GPP) measured at flux tower as a function of (a) the MERIS terrestrial chlorophyll index (MTCI), (b) the product of MTCI and land surface temperature (MODIS LST); (c) the product of MTCI and photosynthetically active radiation (PAR); (d) the product of MTCI and fraction of absorbed photosynthetically active radiation (MODIS *f*PAR); (e) the product of MTCI, MODIS *f*PAR and PAR; and (f) the MODIS GPP product (MOD17). All values are taken from the growing season, defined as the period when GPP is >0 gC $m^{-2}$ $day^{-1}$ and air temperature is >5°C.

the difference in the slope between sites was not as pronounced (Table 3 and Figure 6).

## 4. Discussion

[31] This study is the first to investigate the potential of a satellite-derived, chlorophyll-based VI model for peatland $CO_2$ flux estimation. We expected that chlorophyll-based models, developed using the LUE concept of *Monteith* [1972], would provide good estimations of peatland GPP given that both APAR and LUE are thought to be closely related to the amount of chlorophyll in a plant canopy [*Gitelson et al.*, 2006; *Sellers et al.*, 1992].

[32] There were clear differences in annual maximum GPP both between sites and sometimes between years at the same site. The similarities in the values of the *f*PAR and PAR components of the LUE model between the two sites and between years, suggested that differences in peak GPP were largely a function of the differences in LUE between the two peatlands. This finding is consistent with the differences in nutrient conditions and in the dominant plant functional types between the two peatlands [*Glenn et al.*, 2006]. In a study of species variation in LUE, *Gower et al.* [1999] reported lower LUE for boreal evergreen vegetation, such as that found at Mer Bleue, than for boreal deciduous species, which are more commonly found at the more nutrient-rich Western Peatland site. GPP and LUE were greatly reduced at the Mer Bleue peatland during the summer of 2003, in comparison to the other years studied, thought to be a consequence of low rainfall and thus a lower water table. These patterns concur with a number of studies, which have reported a decrease in the physiological function rates of $CO_2$ uptake in peatland vegetation in response to a lowering of the water table [e.g., *Strack and Waddington*, 2007; *Waddington et al.*, 1998].

[33] The MTCI was able to track the seasonal patterns of plant photosynthetic activity, expressed as GPP, at both peatland sites. Although both peatlands contain evergreen vegetation, the leaves undergo a color change from brown to green during the spring as a consequence of increases in foliar chlorophyll [*Moore et al.*, 2006]. Since most of the new vegetation growth (i.e., new deciduous tissues and leaves on shrubs) occurs from late May onwards, *Moore et al.* [2006] suggest that most of the increases in peat-

land spring photosynthesis at Mer Bleue can be attributed to existing plant tissue that were present at the beginning of the year. Consequently our results suggest that, at least at the Mer Bleue peatland, the MTCI may be responding to both changes in foliar chlorophyll and new vegetation growth, with the former likely to be dominating the change in MTCI earlier in the year.

[34] The MTCI was found to correlate strongly with GPP at both sites and for the majority of the years studied, with the exception of 2003 at Mer Bleue. *Harris and Dash* [2010] also reported significant linear relationships between the MTCI and EC tower estimated GPP across a number of North American ecosystems.

[35] Despite the LST actually being a measure of surface temperature, the LST was significantly correlated with air temperature and sometimes with water table depth. However, the addition of LST to the MTCI model did not lead to marked improvements in overall model performance for either peatland. One of the primary reasons for this was that the strength of relationship between LST and GPP, for a number of individual years and when all years were combined by site, was significant but relatively weak ($r^2 = 0.35$ at Mer Bleue and $r^2 = 0.38$ at the Western Peatland). Although both air temperature and LST are correlated with peatland GPP, the main driver of peatland photosynthetic activity is the soil temperature and of particular importance for shrubs and vascular vegetation in general, is the temperature at the depth of the rooting zone (~10 cm) [*Moore et al.*, 2006]. Temperatures at the bog surface are often higher than those deeper in the peat, especially during the early period of spring growth when the surface temperature is close to or warmer than the air temperature, whereas soil temperatures at the rooting zone are much cooler and deeper soil may remain frozen. Peatland air and surface temperatures, and thus LST, can also fluctuate widely throughout the growing season, whereas soil temperatures at depth often change in a more controlled manner [*Moore et al.*, 2006]. As a consequence LST may not always be representative of the actual temperature controls exerted on peatland photosynthetic processes. However, the interpretation of our LST results is further complicated as changes in air and surface temperature can also be indicative of changes in the vapor pressure deficit (VPD). LST has been shown to be closely related to VPD for a range of different ecosystems [*Granger*, 2000; *Hashimoto et al.*, 2008; *Sims et al.*, 2008] and thus measures of LST can been used as an indicator of vegetation drought stress. Such a relationship between VPD and LST may be the primary reason why the strongest correlations between LST and GPP were observed at Mer Bleue during 2003, when precipitation was below average (Figure 2a) and VPD higher than for any of the other time periods studied (results not shown). As a consequence, under conditions of vegetation "stress" LST may have the potential to improve model performance. The lack of an overall improvement in model performance, with the addition of LST, is in contrast to those of others, such as *Sims et al.* [2008], who found that the addition of LST to their greenness GPP model (based on the use of MODIS EVI data), considerably improved model results. These differences can be explained by the different nature in which photosynthesis responds to changes in environmental variables within different ecosystems, but also by the way in which the growing season was defined in the present study. The 5°C limit on the use of data in all regression models in the current study, evoked to avoid the presence of "artificial" seasonal patterns caused by the onset of snowmelt and snow fall, meant that a number of data points at the start and end of the growing season may have been omitted. In the absence of other environmental stressors (e.g., low precipitation or nutrient deficiency), temperature has a weaker control over GPP during the summer months but a much stronger influence at the beginning and end of the growing season. Consequently, when a greater range of values are used, the correlation between GPP and LST becomes stronger (results not shown). While the addition of LST to the MTCI model may not necessarily improve model performance during the active growing season, as shown in this study, LST may improve the ability of the model to estimate the timing of the inactive photosynthetic period, pre and prior to the growing season, especially for evergreen vegetation [*Sims et al.*, 2008]. However, the differences in the surface temperature and soil temperatures at rooting depth still remain a potential barrier to accurately predicting the onset of peatland photosynthesis using LST.

[36] The lack of a strong significant correlation between GPP and PAR is thought to be a primary reason why the addition of PAR to the MTCI model often resulted in a weaker correlation with GPP than when using the MTCI model alone (Table 2). Low light compensation and saturation points of *Sphagnum* mosses (55–500 $\mu$mol $m^{-2}$ $s^{-1}$) [*Titus and Wagner*, 1984] and shrub leaves at Mer Bleue (600–900 $\mu$mol $m^{-2}$ $s^{-1}$) [*Small*, 1972] may be partially responsible for this weak correlation as linear relationships between photosynthesis and PAR are only observable early and late in the growing season (data not shown). Furthermore, the relationship between PAR and GPP is not only controlled by the amount of PAR that reaches the canopy but also the fraction of this radiation that is diffuse, as diffuse radiation allows radiation to be spread more evenly throughout the plant canopy, thereby reducing light saturation and increasing overall photosynthetic capacity. *Moore et al.* [2006] reported similarly weak but significant correlations between daily rates of GPP and PAR ($r^2 = 0.19$, $p < 0.001$) at Mer Bleue using 5 years of data. *Sims et al.* [2008] also noted that the addition of PAR to a GPP model based solely on the EVI, did not improve correlations with GPP across a variety of ecosystems and in some cases the model performance was reduced, although in contrast, a recent study by *Schubert et al.* [2010] reported stronger correlations between GPP and the product of EVI and PPFD (photosynthetic photon flux density) than between GPP and the product of EVI and temperature, at two Swedish peatlands.

[37] In general, the addition of *f*PAR to the basic MTCI model only slightly improved the correlation with GPP at both sites, although the product of MTCI and *f*PAR was able to explain 13% more of the variation in GPP than the simple MTCI model at Mer Bleue during 2003. This is thought to be a consequence of GPP being more strongly correlated with *f*PAR than MTCI during this time period (Table 2). Although *f*PAR and MTCI are correlated, because canopy growth is inherently linked to photosynthesis, which is in turn related to the presence of chlorophyll, there are also clear differences between these variables. The results suggest that when plant water availability is reduced, as it

was at Mer Bleue during the summer of 2003, the seasonal pattern of carbon uptake is not necessarily altered, even though the actual rate of uptake is reduced. As a consequence *f*PAR remains strongly correlated with GPP, but chlorophyll content, inferred from the MTCI, appears to have less influence over photosynthetic processes under such conditions.

[38] Of all the models tested, the product of MTCI, *f*PAR and PAR was able to explain the most variation in peatland GPP, for both sites and all years tested (Table 3). The MTCI, *f*PAR, PAR model represents a "green" canopy LUE model in so much as the inclusion of MTCI, as an indicator of canopy chlorophyll, within a LUE type model, ensures that the APAR component of the LUE model (i.e., *f*PAR x PAR) relates specifically to the photosynthetic components of the plant canopy i.e., the parts of the canopy that are actually photosynthesising. Only the PAR that is absorbed by chlorophyll is responsible for photosynthesis. Several recent studies have attempted to partition the plant canopy into photosynthetic and non-photosynthetic components either empirically [e.g., *Xiao et al.*, 2004a; 2004b] or via the use of radiative transfer models to improve satellite-based estimates of GPP [e.g., *Zhang et al.*, 2005; 2009]. It is interesting to note that in our study, the greatest improvement in GPP estimation, using the product of MTCI, *f*PAR and PAR, was seen at the Western Peatland site. The model was able to explain almost 15% more of the variation in GPP than the MODIS GPP LUE model, which does not partition the canopy into photosynthetic and non-photosynthetic components (Table 3). The explanation for this may lie in the fact that the Western Peatland is a treed peatland, containing both evergreen and deciduous species. At the Western Peatland, the difference between *f*PAR and the *f*PAR actually able to photosynthesise will be substantially more than at the Mer Bleue site, where trees are small and coverage is sparse, thus the impact of partitioning the *f*PAR by using the MTCI is likely to be far more pronounced. For a deciduous forest, *Zhang et al.* [2005] reported large differences between the *f*PAR of the canopy and the *f*PAR of only the photosynthetic components, the extent of which varied significantly over time.

[39] Our results also show site-specific slopes in the relation of GPP for all models tested, including the MODIS GPP product, albeit to a lesser extent than the models developed from the MTCI. The slopes of the relationships were in all cases higher at the Western Peatland site than at Mer Bleue (Figure 6). It is not clear from our results what the main cause of the difference in slope is. One explanation could be the influence of canopy structure on the retrieval of the MTCI. However, the relationship between chlorophyll content and indices developed from the red edge region of the electromagnetic spectrum, have often been shown to be insensitive to differences in canopy structure [e.g., *Gitelson et al.*, 1996]. Furthermore, this explanation would not explain why the slope of the MODIS GPP regression line was also higher at the Western Peatland site. An alternative explanation could be associated with the impact of shadowing in environments where conical-shaped trees are located in close proximity to one another, as at the Western Peatland, thereby reducing overall reflectance from the plant canopy. Shadowing is likely to result in a proportionally greater reduction in reflectance in the NIR than in the Red regions of the electromagnetic spectrum. This would mean that for a given value of GPP the MTCI value would be lower in a shadowed canopy than in a non-shadowed canopy thus effectively increasing the slope of the linear relationship between MTCI and GPP. The slope of the relationships with GPP may also be affected by differences in the LUE of the peatland vegetation, i.e., for the same amount of chlorophyll, as indicated by the MTCI, the GPP is higher at the Western Peatland than at Mer Bleue. This explanation is consistent with the higher LUE values recorded at the Western Peatland and may also explain why the slope of the relationship with GPP at Mer Bleue is much lower during the drier year of 2003 than any of the other years. Both the MTCI and *f*PAR are able to track patterns in GPP, but such products often provide a measure of potential rather than actual photosynthesis [*Garbulsky et al.*, 2011]. Consequently they are unable to mirror reductions in carbon uptake, which may not be immediately reflected in changes in vegetation physiology. At the Mer Bleue site, seasonal values of *f*PAR and MTCI were similar for all years studied. Consequently during 2003, MTCI values did not reflect the reduction that was observed in GPP, which resulted in the observed lower slope of the GPP relationship (Figure 6a). A similarly low slope of the GPP relationship for Mer Bleue in 2003 was observed for the MODIS GPP model, which includes a LUE component. This may suggest that the impact of low moisture availability on LUE may not be fully accounted for by the vapor pressure deficit (VPD) scalar in the MODIS GPP model. A number of previous studies using spectral indices-based models have suggested that parameters such as mean annual nighttime temperature [*Sims et al.*, 2008] or peak LAI [*Lindroth et al.*, 2008] may be used to account for site-specific relationships and thus enable scaling of GPP using satellite data. However, the current paucity of peatland EC data and the relatively short archive of MERIS data (i.e., from 2003 onwards) preclude such investigations in this study. To facilitate a fuller explanation of the current findings, future research efforts should be directed toward detailed studies investigating both the influence of peatland canopy structure and vegetation physiology on spectral reflectance and photosynthetic processes under varying temperature and moisture regimes.

[40] While the results of the study have shown great promise, there are a number of issues that must be considered when utilizing EC tower data and coarse resolution remotely sensed data (e.g., 1 km) to estimate GPP for peatland landscapes. The primary issue is related to how representative a 1 km pixel is, of peatland vegetation within the footprint of the flux tower. In this study, every effort has been made to select pixels that are thought to be representative of the peatland vegetation within the flux tower footprint. Values of the MTCI extracted from the full resolution 300 m MERIS pixel located nearest to each of the flux towers, were consistent with those obtained from the corresponding 1 km data. As ~80% of the flux measured by EC towers often comes from within 200 m of the tower site [e.g., *Connolly et al.*, 2009; *Lund et al.*, 2007], we assume that the 1 km tower pixels provide a reasonable representation of the site conditions. However, there are a number of potential errors associated with such an assumption. First, the flux tower footprint is not a static entity. The actual size and shape of the footprint largely depends upon wind speed,

direction and surface roughness [*Schmid*, 2002], all of which may vary spatially and temporarily. Second, the geolocation accuracy of the satellite data is not perfect. The error in the absolute location accuracy of the MERIS data varies between 160 m and 230 m, dependent on year of data acquisition [*Goryl and Saunier*, 2004]. Consequently there is the potential for a scale mismatch between the flux tower footprint and the MERIS pixels used. The implications of such a scenario would be greatest for the Mer Bleue peatland, where heterogeneity in MTCI values within the 1 km MTCI pixel, appears to be greatest. A somewhat related issue is the development of MTCI-based models using data from multiple sensors. Where it was necessary to develop models using data from both the MERIS and MODIS sensors, the artifacts of, and differences in, viewing geometry, geolocation accuracy of pixels, and the resampling and/or compositing techniques of the two sensors, are such that pixels may not always be perfectly co-registered. The implications of such a mismatch are again greatest when monitoring heterogeneous landscapes. One way to avoid such problems would be to utilize remote sensing data from the same satellite sensor. The MERIS global vegetation index (MGVI) is a standard level 2 (L2) product that estimates *f*PAR from MERIS data [*Gobron et al.*, 1999], although at the time of this study MGVI composites at appropriate spatial and temporal resolution were unavailable.

[41] One possible future solution to overcome both the problems of peatland spatial heterogenity and the unwanted artifacts associated with combining data from different sensor platforms, is to utilize data obtained from the forthcoming Sentinel suite of satellites, due to be launched by the European Space Agency in 2013. The Ocean and Land Color Instrument (OLCI) on board Sentinel-3, will enable the routine generation and compositing of both MTCI and MGVI data products at the full 300 m spatial resolution, thus both products will be routinely available from the same sensor at a higher spatial resolution than is currently possible. Furthermore, Sentinel-2, with its large swath width (290 km) and frequent revisit period (~5 days at midlatitudes), will facilitate the generation of MTCI data with an unprecedented 20 m spatial resolution. Such information is essential for spatially explicit monitoring of peatland carbon dynamics.

## 5. Conclusion

[42] Our results have shown that simple MTCI-based models can be used for estimates of inter- and intra-annual variability in peatland GPP. The MTCI is itself a good indicator of peatland GPP and compared favorably with the more complex MODIS GPP product on a site specific basis. The incorporation of MTCI into a light use efficiency type model, by means of partitioning the fraction of photosynthetic material within a plant canopy, showed most promise for treed peatlands, outperforming all other models, including the MODIS GPP product. Although a number of the MTCI-based models work well for individual sites, research is ongoing in order to predict the variations in the slope of the relationship between MTCI-based models and GPP and to fully account for the down regulation in carbon uptake, which may occur under moisture limiting conditions. More work is also needed to fully explore the efficacy of this technique across other peatlands and, where possible, to utilize longer time series of data for full model development and validation. Our results show great promise, although future research should also concentrate on understanding the potential of the forthcoming ESA Sentinel missions for improved spatial characterization of peatland fluxes. We suggest that the MTCI may ultimately facilitate improved quantification of the temporal and spatial dynamics of peatland carbon fluxes.

[43] **Acknowledgments.** The authors wish to thank the NERC Earth Observation Data Centre (NEODC) for MTCI composite data, ESA for MERIS full resolution data (Project ID- 3976) and the Oak Ridge National Laboratory (ORNL) Distributed Active Archive Center (DAAC) for MODIS data. Data for the MTCI composites were provided by ESA and were processed by Infoterra Ltd, United Kingdom. We also wish to thank P. M. Lafleur, L. B. Flanagan and the Fluxnet Canada Research Network/ Canadian Carbon Programme for providing the flux tower data. The anonymous referees are also thanked for their comments, which helped to improve the manuscript.

## References

Arora, V. K., and G. J. Boer (2005), A parameterization of leaf phenology for the terrestrial ecosystem component of climate models, *Global Change Biol.*, *11*, 39–59, doi:10.1111/j.1365-2486.2004.00890.x.

Bubier, J. L. (1995), The relationship of vegetation to methane emission and hydrochemical gradients in northern peatlands, *J. Ecol.*, *83*(3), 403–420, doi:10.2307/2261594.

Bubier, J. L., B. N. Rock, and P. M. Crill (1997), Spectral reflectance measurements of boreal wetland and forest mosses, *J. Geophys. Res.*, *102*(D24), 29,483–29,494, doi:10.1029/97JD02316.

Bubier, J., T. Moore, K. Savage, and P. Crill (2005), A comparison of methane flux in a boreal landscape between a dry and a wet year, *Global Biogeochem. Cycles*, *19*, GB1023, doi:10.1029/2004GB002351.

Connolly, J., N. T. Roulet, J. W. Seaquist, N. M. Holden, P. M. Lafleur, E. R. Humphreys, B. W. Heumann, and S. M. Ward (2009), Using MODIS derived *f* PAR with ground based flux tower measurements to derive the light use efficiency for two Canadian peatlands, *Biogeosciences*, *6*(2), 225–234, doi:10.5194/bg-6-225-2009.

Curran, P. J., J. Dash, T. Lankester, and S. Hubbard (2007), Global composites of the MERIS terrestrial chlorophyll index, *Int. J. Remote Sens.*, *28*(17), 3757–3758, doi:10.1080/01431160600639685.

Dash, J., and P. J. Curran (2004), The MERIS terrestrial chlorophyll index, *Int. J. Remote Sens.*, *25*(23), 5403–5413, doi:10.1080/0143116042000274015.

Dise, N. B., E. Gorham, and E. S. Verry (1993), Environmental factors controlling methane emissions from peatlands in northern Minnesota, *J. Geophys. Res.*, *98*(D6), 10,583–10,594, doi:10.1029/93JD00160.

Environment Canada (2006), *Canadian Climate Normals or Averages 1971–2000*, http://climate.weatheroffice.gc.ca/climate_normals/index_e.html [accessed February 2011].

Frolking, S., N. T. Roulet, T. R. Moore, P. M. Lafleur, J. L. Bubier, and P. M. Crill (2002), Modeling seasonal to annual carbon balance of Mer Bleue Bog, Ontario, Canada, *Global Biogeochem. Cycles*, *16*(3), 1030, doi:10.1029/2001GB001457.

Garbulsky, M. F., J. Peñuelas, J. Gamon, Y. Inoue, and I. Filella (2011), The photochemical reflectance index (PRI) and the remote sensing of leaf, canopy and ecosystem radiation use efficiencies: A review and meta-analysis, *Remote Sens. Environ.*, *115*(2), 281–297, doi:10.1016/j.rse.2010.08.023.

Gitelson, A. A., M. N. Merzylak, and H. K. Lichtenthaler (1996), Detection of red edge position and chlorophyll content by reflectance measurements near 700 nm, *J. Plant Physiol.*, *148*, 501–508.

Gitelson, A. A., A. Viña, V. Ciganda, D. C. Rundquist, and T. J. Arkebauer (2005), Remote estimation of canopy chlorophyll content in crops, *Geophys. Res. Lett.*, *32*, L08403, doi:10.1029/2005GL022688.

Gitelson, A. A., A. Viña, S. B. Verma, D. C. Rundquist, T. J. Arkebauer, G. Keydan, B. Leavitt, V. Ciganda, G. G. Burba, and A. E. Suyker (2006), Relationship between gross primary production and chlorophyll content in crops: Implications for the synoptic monitoring of vegetation productivity, *J. Geophys. Res.*, *111*, D08S11, doi:10.1029/2005JD006017.

Gitelson, A. A., A. Viña, J. G. Masek, S. B. Verma, and A. E. Suyker (2008), Synoptic monitoring of gross primary productivity of maize

using Landsat data, *IEEE Geosci. Remote Sens. Lett.*, *5*(2), 133–137, doi:10.1109/LGRS.2008.915598.

Glenn, A. J., L. B. Flanagan, K. H. Syed, and P. J. Carlson (2006), Comparison of net ecosystem $CO_2$ exchange in two peatlands in western Canada with contrasting dominant vegetation, *Sphagnum* and *Carex*, *Agric. For. Meteorol.*, *140*(1–4), 115–135, doi:10.1016/j.agrformet.2006.03.020.

Gobron, N., B. Pinty, M. Verstraete, and Y. Govaerts (1999), The MERIS Global Vegetation Index (MGVI): Description and preliminary application, *Int. J. Remote Sens.*, *20*(9), 1917–1927, doi:10.1080/014311699212542.

Goryl, P., and S. Saunier (2004), *MERIS Absolute Geolocation Status*, ESA Product Control Service documentation, http://earth.esa.int/pcs/envisat/meris/documentation/.

Gower, S. T., C. J. Kucharik, and J. M. Norman (1999), Direct and indirect estimation of leaf area index, $f_{APAR}$, and net primary production of terrestrial ecosystems, *Remote Sens. Environ.*, *70*(1), 29–51, doi:10.1016/S0034-4257(99)00056-5.

Granger, R. J. (2000), Satellite-derived estimates of evapotranspiration in the Gediz basin, *J. Hydrol.*, *229*, 70–76, doi:10.1016/S0022-1694(99)00200-0.

Harris, A., and R. G. Bryant (2009), Northern peatland vegetation and the carbon cycle: A remote sensing approach, in *Carbon Cycling in Northern Peatlands*, edited by A. J. Baird et al., pp. 79–98, AGU, Washington, D. C.

Harris, A., and J. Dash (2010), The potential of the MERIS terrestrial chlorophyll index for carbon flux estimation, *Remote Sens. Environ.*, *114*(8), 1856–1862, doi:10.1016/j.rse.2010.03.010.

Hashimoto, H., J. L. Dungan, M. A. White, F. Yang, A. R. Michaelis, S. W. Running, and R. R. Nemani (2008), Satellite-based estimation of surface vapor pressure deficits using MODIS land surface temperature data, *Remote Sens. Environ.*, *112*(1), 142–155, doi:10.1016/j.rse.2007.04.016.

Heinsch, F. A., et al. (2003), User's Guide GPP and NPP (MOD17A2/A3) Products, NASA MODIS Land Algorithm, Version 2.0, 57 pp., Numer. Terradyn. Simul. Group, Missoula, Mont. (Available at http://www.ntsg.umt.edu/sites/ntsg.umt.edu/files/modis/MOD17UsersGuide.pdf.).

Heinsch, F. A., et al. (2006), Evaluation of remote-sensing-based terrestrial productivity from MODIS using regional tower eddy flux network observations, *IEEE Trans. Geosci. Remote Sens.*, *44*(7), 1908–1925, doi:10.1109/TGRS.2005.853936.

Jago, R. A., M. E. J. Cutler, and P. J. Curran (1999), Estimating canopy chlorophyll concentration from field and airborne spectra, *Remote Sens. Environ.*, *68*(3), 217–224, doi:10.1016/S0034-4257(98)00113-8.

Krankina, O. N., D. Pflugmacher, M. Friedl, W. B. Cohen, P. Nelson, and A. Baccini (2008), Meeting the challenge of mapping peatlands with remotely sensed data, *Biogeosciences*, *5*(6), 1809–1820, doi:10.5194/bg-5-1809-2008.

La Puma, I. P., T. E. Philippi, and S. F. Oberbauer (2007), Relating NDVI to ecosystem $CO_2$ exchange patterns in response to season length and soil warming manipulations in arctic Alaska, *Remote Sens. Environ.*, *109*(2), 225–236, doi:10.1016/j.rse.2007.01.001.

Lachenbruch, P. A., and M. R. Mickey (1968), Estimation of error rates in discriminant analysis, *Technometrics*, *10*, 1–11, doi:10.2307/1266219.

Lafleur, P. M., N. T. Roulet, and S. Admiral (2001), Annual cycle of $CO_2$ exchange at a bog peatland, *J. Geophys. Res.*, *106*(D3), 3071–3081, doi:10.1029/2000JD900588.

Lafleur, P. M., N. T. Roulet, J. L. Bubier, S. Frolking, and T. R. Moore (2003), Interannual variability in the peatland-atmosphere carbon dioxide exchange at an ombrotrophic bog, *Global Biogeochem. Cycles*, *17*(2), 1036, doi:10.1029/2002GB001983.

Lafleur, P. M., R. A. Hember, S. W. Admiral, and N. T. Roulet (2005), Annual and seasonal variability in evapotranspiration and water table at a shrub-covered bog in southern Ontario, Canada, *Hydrol. Processes*, *19*(18), 3533–3550, doi:10.1002/hyp.5842.

Laine, A., M. Sottocornola, G. Kiely, K. Byrne, D. Wilson, and E. Tuittila (2006), Estimating net ecosystem exchange in a patterned ecosystem: Example from blanket bog, *Agric. For. Meteorol.*, *138*(1–4), 231–243, doi:10.1016/j.agrformet.2006.05.005.

Lindroth, A., et al. (2008), Leaf area index is the principal scaling parameter for both gross photosynthesis and ecosystem respiration of northern deciduous and coniferous forests, *Tellus, Ser. B*, *60*(2), 129–142, doi:10.1111/j.1600-0889.2007.00330.x.

Liu, J., J. M. Chen, J. Cihlar, and W. M. Park (1997), A process-based boreal ecosystem productivity simulator using remote sensing inputs, *Remote Sens. Environ.*, *62*(2), 158–175, doi:10.1016/S0034-4257(97)00089-8.

Lund, M., A. Lindroth, T. R. Christensen, and L. Ström (2007), Annual $CO_2$ balance of a temperate bog, *Tellus, Ser. B*, *59*(5), 804–811, doi:10.1111/j.1600-0889.2007.00303.x.

Monteith, J. L. (1972), Solar radiation and productivity in tropical ecosystems, *J. Appl. Ecol.*, *9*(3), 747–766, doi:10.2307/2401901.

Moore, P. D. (1998), The future of cool temperate bogs, *Environ. Conserv.*, *29*, 3–20.

Moore, T. R., J. L. Bubier, S. E. Frolking, P. M. Lafleur, and N. T. Roulet (2002), Plant biomass and production and $CO_2$ exchange in an ombrotrophic bog, *J. Ecol.*, *90*(1), 25–36, doi:10.1046/j.0022-0477.2001.00633.x.

Moore, T. R., P. M. Lafleur, D. M. I. Poon, B. W. Heumann, J. W. Seaquist, and N. T. Roulet (2006), Spring photosynthesis in a cool temperate bog, *Global Change Biol.*, *12*(12), 2323–2335, doi:10.1111/j.1365-2486.2006.01247.x.

Myneni, R., Y. Knyazikhin, J. Glassy, P. Votava, and N. Shabanov (2003), User's guide: FPAR, LAI (ESDT: MOD15A2) 8-day Composite NASA MODIS Land Algorithm, 17 pp., Boston Univ., Boston, Mass. (Available at http://cybele.bu.edu/modismisr/products/modis/userguide.pdf.).

Nouvellon, Y., D. L. Seen, S. Rambal, A. Bégué, M. S. Moran, Y. Kerr, and J. Qi (2000), Time course of radiation use efficiency in a shortgrass ecosystem: Consequences for remotely sensed estimation of primary production, *Remote Sens. Environ.*, *71*(1), 43–55, doi:10.1016/S0034-4257(99)00063-2.

Post, W. M., W. R. Emanuel, P. J. Zinke, and A. G. Stangenberger (1982), Soil carbon pools and world life zones, *Nature*, *298*(5870), 156–159, doi:10.1038/298156a0.

Prince, S. D., and S. N. Goward (1995), Global primary production: A remote sensing approach, *J. Biogeogr.*, *22*, 815–835, doi:10.2307/2845983.

Rahman, A. F., D. A. Sims, V. D. Cordova, and B. Z. El-Masri (2005), Potential of MODIS EVI and surface temperature for directly estimating per-pixel ecosystem C fluxes, *Geophys. Res. Lett.*, *32*, L19404, doi:10.1029/2005GL024127.

Ruimy, A., B. Saugier, and G. Dedieu (1994), Methodology for the estimation of net primary production from remotely sensed data, *J. Geophys. Res.*, *99*(D3), 5263–5283, doi:10.1029/93JD03221.

Running, S. W., R. R. Nemani, F. A. Heinsch, M. S. Zhao, M. Reeves, and H. Hashimoto (2004), A continuous satellite-derived measure of global terrestrial primary production, *BioScience*, *54*, 547–560, doi:10.1641/0006-3568(2004)054[0547:ACSMOG]2.0.CO;2.

Schmid, H. P. (2002), Footprint modeling for vegetation atmosphere exchange studies: A review and perspective, *Agric. For. Meteorol.*, *113*(1–4), 159–183, doi:10.1016/S0168-1923(02)00107-7.

Schubert, P., L. Eklundh, M. Lund, and M. Nilsson (2010), Estimating northern peatland $CO_2$ exchange from MODIS time series data, *Remote Sens. Environ.*, *114*(6), 1178–1189, doi:10.1016/j.rse.2010.01.005.

Schwalm, C. R., et al. (2006), Photosynthetic light use efficiency of three biomes across an east–west continental-scale transect in Canada, *Agric. For. Meteorol.*, *140*(1–4), 269–286, doi:10.1016/j.agrformet.2006.06.010.

Sellers, P. J., J. A. Berry, G. J. Collatz, C. B. Field, and F. G. Hall (1992), Canopy reflectance, photosynthesis, and transpiration. 3. A reanalysis using improved leaf models and a new canopy integration scheme, *Remote Sens. Environ.*, *42*(3), 187–216, doi:10.1016/0034-4257(92)90102-P.

Sims, D. A., H. Y. Luo, S. Hastings, W. C. Oechel, A. F. Rahman, and J. A. Gamon (2006a), Parallel adjustments in vegetation greenness and ecosystem $CO_2$ exchange in response to drought in a Southern California chaparral ecosystem, *Remote Sens. Environ.*, *103*(3), 289–303, doi:10.1016/j.rse.2005.01.020.

Sims, D. A., et al. (2006b), On the use of MODIS EVI to assess gross primary productivity of North American ecosystems, *J. Geophys. Res.*, *111*, G04015, doi:10.1029/2006JG000162.

Sims, D. A., et al. (2008), A new model of gross primary productivity for North American ecosystems based solely on the enhanced vegetation index and land surface temperature from MODIS, *Remote Sens. Environ.*, *112*(4), 1633–1646, doi:10.1016/j.rse.2007.08.004.

Small, E. (1972), Photosynthesis rates in relation to nitrogen recycling as an adaptation to nutrient deficiency in peat bog plants, *Can. J. Bot.*, *50*, 2227–2233, doi:10.1139/b72-289.

Smith, L. C., G. M. MacDonald, A. A. Velichko, D. W. Beilman, O. K. Borisova, K. E. Frey, K. V. Kremenetski, and Y. Sheng (2004), Siberian peatlands a net carbon sink and global methane source since the early Holocene, *Science*, *303*(5656), 353–356, doi:10.1126/science.1090553.

Soegaard, H., N. O. Jensen, E. Boegh, C. B. Hasager, K. Schelde, and A. Thomsen (2003), Carbon dioxide exchange over agricultural landscape using eddy correlation and footprint modelling, *Agric. For. Meteorol.*, *114*(3–4), 153–173, doi:10.1016/S0168-1923(02)00177-6.

Sonnentag, O., J. M. Chen, N. T. Roulet, W. Ju, and A. Govind (2008), Spatially explicit simulation of peatland hydrology and carbon dioxide exchange: Influence of mesoscale topography, *J. Geophys. Res.*, *113*, G02005, doi:10.1029/2007JG000605.

Strack, M., and J. M. Waddington (2007), Response of peatland carbon dioxide and methane fluxes to a water table drawdown experiment, *Global Biogeochem. Cycles*, *21*, GB1007, doi:10.1029/2006GB002715.

Sun, P., A. Grignetti, S. Liu, R. Casacchia, R. Salvatori, F. Pietrini, F. Loreto, and M. Centritto (2008), Associated changes in physiological parameters and spectral reflectance indices in olive (*Olea europaea L.*) leaves in response to different levels of water stress, *Int. J. Remote Sens.*, *29*(6), 1725–1743, doi:10.1080/01431160701373754.

Syed, K. H., L. B. Flanagan, P. J. Carlson, A. J. Glenn, and K. E. Van Gaalen (2006), Environmental control of net ecosystem $CO_2$ exchange in a treed, moderately rich fen in northern Alberta, *Agric. For. Meteorol.*, *140*(1–4), 97–114, doi:10.1016/j.agrformet.2006.03.022.

Titus, J. E., and D. J. Wagner (1984), Carbon balance for two *Sphagnum* mosses: Water balance resolves a physiological paradox, *Ecology*, *65*(6), 1765–1774, doi:10.2307/1937772.

Waddington, J. M., T. J. Griffis, and W. R. Rouse (1998), Northern Canadian wetlands: Net ecosystem $CO_2$ exchange and climatic change, *Clim. Change*, *40*(2), 267–275, doi:10.1023/A:1005468920206.

Wang, S. S., R. F. Grant, D. L. Verseghy, and T. A. Black (2002), Modelling carbon dynamics of boreal forest ecosystems using the Canadian Land Surface Scheme, *Clim. Change*, *55*(4), 451–477, doi:10.1023/A:1020780211008.

Wylie, B. K., D. A. Johnson, E. Laca, N. Z. Saliendra, T. G. Gilmanov, B. C. Reed, L. L. Tieszen, and B. B. Worstell (2003), Calibration of remotely sensed, coarse resolution NDVI to $CO_2$ fluxes in a sagebrush-steppe ecosystem, *Remote Sens. Environ.*, *85*(2), 243–255, doi:10.1016/S0034-4257(03)00004-X.

Xiao, X., D. Hollinger, J. Aber, M. Goltz, E. A. Davidson, Q. Zhang, and B. Moore III (2004a), Satellite-based modeling of gross primary production in an evergreen needleleaf forest, *Remote Sens. Environ.*, *89*(4), 519–534, doi:10.1016/j.rse.2003.11.008.

Xiao, X., Q. Zhang, B. Braswell, S. Urbanski, S. Boles, S. Wofsy, B. Moore, and D. Ojima (2004b), Modeling gross primary production of temperate deciduous broadleaf forest using satellite images and climate data, *Remote Sens. Environ.*, *91*(2), 256–270, doi:10.1016/j.rse.2004.03.010.

Yurova, A. Y., and H. Lankreijer (2007), Carbon storage in the organic layers of boreal forest soils under various moisture conditions: A model study for Northern Sweden sites, *Ecol. Modell.*, *204*(3–4), 475–484, doi:10.1016/j.ecolmodel.2007.02.003.

Yurova, A., A. Wolf, J. Sagerfors, and M. Nilsson (2007), Variations in net ecosystem exchange of carbon dioxide in a boreal mire: Modeling mechanisms linked to water table position, *J. Geophys. Res.*, *112*, G02025, doi:10.1029/2006JG000342.

Zhang, Q. Y., X. M. Xiao, B. Braswell, E. Linder, F. Baret, and B. Moore (2005), Estimating light absorption by chlorophyll, leaf and canopy in a deciduous broadleaf forest using MODIS data and a radiative transfer model, *Remote Sens. Environ.*, *99*(3), 357–371, doi:10.1016/j.rse.2005.09.009.

Zhang, Q. Y., E. M. Middleton, H. A. Margolis, G. G. Drolet, A. A. Barr, and T. A. Black (2009), Can a satellite-derived estimate of the fraction of PAR absorbed by chlorophyll ($FAPAR_{chl}$) improve predictions of light-use efficiency and ecosystem photosynthesis for a boreal aspen forest?, *Remote Sens. Environ.*, *113*(4), 880–888, doi:10.1016/j.rse.2009.01.002.

Zhao, M., S. W. Running, and R. R. Nemani (2006), Sensitivity of Moderate Resolution Imaging Spectroradiometer (MODIS) terrestrial primary production to the accuracy of meteorological reanalyses, *J. Geophys. Res.*, *111*, G01002, doi:10.1029/2004JG000004.

J. Dash, School of Geography, University of Southampton, Highfield, Southampton SO17 1BJ, UK.

A. Harris, Geography Department, School of Environment and Development, University of Manchester, Oxford Road, Manchester M13 9PL, UK. (angela.harris@manchester.ac.uk)